EasyChair Preprint

№ 5118

Investigative Study on Fuzzy PID Structures Based on Single-Axis Solar Tracking System

Abraham Amole, Gabriel Ogungbure, Daniel Akinyele, Olakunle Olabode and David Aborisade

March 9, 2021

Investigative Study on Fuzzy PID Structures Based on Single-Axis Solar Tracking System

[1]Amole Abraham O., [2]Ogungbure Gabriel, [3]Akinyele Daniel O., [4]Olabode Olakunle E. and [5]Aborisade David O.
[1,3,4]Department of Electrical, Electronics and Computer Engineering, Bells University of Technology, Ota, Ogun State, Nigeria.
[2,5]Department of Electronic and Electrical Engineering, Ladoke Akintola University of Technology, Ogbomoso, Oyo State, Nigeria.

latidassah@gmail.com, Gabriel.ogungbure@gmail.com, akinyelescholar@gmail.com, 095082@gmail.com, doaborisade@gmail.com

Abstract

The need for alternative energy sources has been a propelling driver pivoting huge investment in the harvesting of solar energy as a means to combat the energy crisis in many sub-Sahara African countries. Efficient harvesting of this energy during the day largely depends on the tracking system employed, which could either be a single or dual-axis. This work explores the structures of Fuzzy Proportional-Integral-Derivative (PID) for controlling the solar tracking system. A direct current (D.C.) motor was modeled as the solar tracking system based on Kirchhoff's laws. The Fuzzy logic of linear and nonlinear structures was used to tune the proposed PID controller while the simulation was done in Matlab/Simulink environment. The sun's trajectory was accurately tracked by the fuzzy (PD+I) and PID controller for 12 hours and mimicked response at a maximum altitude angle of 58.20° with minimal error and quick response. The performance of the proposed system design was evaluated based on the rise time, settling time, overshoot, and peak time as metrics. Results obtained based on the PD+I controller structure outperformed the conventional PID and Fuzzy PI + PD controller structures, with a rise time, settling time, overshoot, and the peak time of 1.15s, 3.15, 3%, and 1.43s, respectively, when subjected to a load of 0.1 Nm.

Keywords: Energy harvesting, PID, Fuzzy-PID structures, solar tracker, Photovoltaic performance, Kirchoff's laws.

1. Introduction

Energy, among other forms of energy is very indispensable to human race most especially in this modern age where virtually all of human activities either at domestic or industrial level rest solely on its availability. It plays a central role in achieving good economic development (Eshun and Amoako-Tuffour, 2016; IEA 2014). The author; Adusei (2014), emphasized that the impact of electricity cut across enhanced security by surveillance system, maintenance of law and order, and stability. High demand for electricity is a major factor causing energy crisis most especially in third world countries like Nigeria (Oyedepo, 2012).

Electrical energy can be harvested from various sources like hydro, thermal, wind, nuclear, biomass, and solar (Bada, 2011; Shaaban and Petirin, 2014). Hydropower, thermal power and other non-renewable sources have been intensively explored over time for production of electricity on a large scale for human usage. However, the energy produced from these sources cannot match energy demanded by various types of consumers (Shaaban and Petirin, 2014), hence the need to explore other alternative energy sources to complement the above-mentioned sources. Renewable energy sources have proven to be viable alternative to combat rising energy crisis in many of these developing countries (Tiwari and Mishra, 2011), of which exploration of solar energy at present is really attracting attention of researchers as viable alternative source in Sub-Saharan Africa due to abundant sunshine (Yilmaz et al., 2015; Abdullahi, 2017). The authors; Panwar, Kaushik and Kothari, 2011 and Roth, Georgiev, and Boudinov (2016) argued that the aggregate sum of energy that is obtainable from solar radiation reaching the earth has been estimated to be more than 7,500 times the total amount of energy primarily consumed annually by the world both for the domestic and industrial purposes.

Solar energy is one of the cleanest forms of energy and is obtain from solar irradiation reaching the earth (Roth, Georgiev, and Boudinov (2016), Owusu and Asumadu-Sarkodie, 2016). Research studies have shown that full utilization of the solar panel potential depends on factors such as climatic conditions, type, and size of the panel, the orientation of the panel (Guaita-Pradas, Marques-Perez, Gallego, and Baldomero, 2019). The orientation of the panel is a central factor to be consider when installing the panel as it determines the amount of solar radiation that will reach the panel surface. However, the sun is not static hence; solar panels need to be rotated to align with sun's movement (Abdallah, 2004), with this approach, maximum energy will be produced. To achieve this in practice, a solar tracking system is employed; it helps to maintain the panel orthogonal position relative to the solar radiation (Li and Lam, 2007 and Liu, et al., 2013). A solar tracker changes the direction of a mounted solar panel in response to the current location of the sun's most intense radiation, this allow

surface of the panel to be exposed to maximum sun intensity right from sunrise to sunset (Liu, et al., 2013, Rahman et al., 2013, El Kadmiri et al., 2015 and Gama et al., 2013). Solar tracking systems can guarantee about 35% increase in the efficiency of energy production on annual basis (Racharla and Rajan, 2017) and its efficiency depends largely on the season, it is higher during winter than any other months of the year (Usta, Akyaszi, and Atlas, 2011). Solar tracking systems could be designed as single-axis or dual trackers, single axis tracker can be horizontal, vertical or tilted single-axis trackers (Louchene, Benmakhlouf and Chaghi, 2007 and Li et al., 2014).

It has been reported that the optimal performance of solar panel depends on precise control of the tracker on which the panel is mounted (Dhanabal et al., 2013 and Bakos, 2006). There are several means of controlling solar tracking system, which ranges from the conventional PID controllers (Mahfouz, Aly, and Salem, 2013, Kiyak and Gol, 2016, and Sahoo, Samanta, and Bhattacharyya, 2018), sliding mode controller [(Merheb, Noura and Bateman, 2015 and Jiang et al., 2018) to intelligent controllers like fuzzy logic (Usta, O. Akyaszi, and I. H. Atlas, 2011, Jiang et al., 2018, and Batayneh, Owais, and Nairoukh, 2013). The work of Mardlijah et al., (2019) control the solar panel using modified type-2 fuzzy sliding mode, the solar panel system was mathematically modeled and the control scheme was designed using the T2FSMC approach that accepts two inputs. Fuzzy rules were defined while system normalized gain was computed using bisection algorithm; the authors concluded that modified T2FSMC outperformed Fuzzy Sliding Mode Control (FSMC).

The tracking time and accuracy of the solar tracker system under varying irradiance and temperature was improved upon by authors in (Kabalci, Calpbinici and Kabalci, 2015, Samantaa, Duttab, and Neogic, 2012, and Chamanpira et al., 2019) based on Fuzzy Gain Scheduling-PID (FGS-PID) controller in the grid-connected mode. Ziegler–Nichols was used for effective tuning of FGS-PID. The simulation results showed that the tracking time and accuracy, 99.17% and 0.12s respectively for Ziegler–Nichols tuned FGS-PID, this was found to be comparatively high relative to what was obtained with ANN, ANFIS, Fuzzy, INC, P&O, PID, and FGSPID methods. Pei et al., (2018) employed permanent magnet synchronous motor for position tracking based on fuzzy PID-variable structure adaptive control, both the state equation of the PMSM and fuzzy-PID variable structure was designed using sliding mode surface to circumvent disturbance and uncertainty effect, fuzzy PID-variable structure adaptive control was found to be comparative better in based on control precision and dynamic performance. This present work employed different structures of Fuzzy-PID for solar tracking system based on single axis.

The rest of this paper was as structured as follows, section 2 focuses on module orientation and tracking, section 3 describes in detail the system description, the mathematical modelling of DC motor and PID-structure, section 4 presents the simulation results obtained while section 5 concludes the study.

2. Solar module orientation and tracking

Solar photovoltaic modules need to be designed in such a manner that they are positioned or oriented in the direction of the "solar window" to capture maximum amount of solar energy at a particular site of interest (Brooks and Dunlop, 2012). The solar window in this case, according to the authors in (Brooks and Dunlop, 2012), refers to a range of solar paths for a particular latitude between the two dates within the year that the sun attains its highest or lowest declination, i.e. the solstices, which usually translates to the longest or shortest days in the year. In a practical sense, the implication of this is that shorter solar paths and days are usually experienced during the winter season, while longer solar paths and days are experienced during the summer season. However, the rainy and the dry seasons are usually experienced in a tropical country like Nigeria. Whether a solar photovoltaic is in the temperature or tropical region, the desire of the designer or engineer is to ensure that it has achieves optimum performance.

The solar module azimuth angle and the tilt angle are two critical angles that determine the orientation of modules (Brooks and Dunlop, 2012). The module azimuth angle may be defined as the direction that the solar photovoltaic module surface is facing measured with the compass heading to due south. In the northern hemisphere, optimal azimuth angle is realized when the solar module is faced due south, i.e. the compass heading is 180° measured clockwise from the north pole., provided there is no shading effect on the module. However, the solar module is tilted facing due north in the southern hemisphere to obtain the optimum azimuth angle. The module tilt angle may be described as the angle between the surface of the solar module and the horizontal plane. Conventionally, the tilt angle is determined by the location's latitude, and by implication, the higher the location's latitude, the higher the chance of achieving maximum energy capture because of the higher optimal tilt angle (Brooks and Dunlop, 2012 and Markvart and Castañer, 2003).

2.1 Fixed tilted photovoltaic modules

It is established that the orientation of solar photovoltaic modules and/or tracking arrangements are part of the factors that determine the "long-term" solar irradiance profiles for increased energy generation (Markvart and Castañer, 2003). A general guideline for optimum solar module inclination for systems in the northern hemisphere, for example, is location's latitude - 15°, latitude +15° and the latitude for summer, winter and annual average, respectively (Markvart and Castañer,

2003). The annual average in this case depicts sites that have little variation in solar insolation per day over the year. However, it is expected that solar insolation will be high for summer months and low for winter months.

The fixed-axis or fixed tilted solar photovoltaic modules can optimize the solar energy capture, but this can be achieved for a limited period of time (Gevorkian, 2012). The arrangement is also regarded as latitude-fixed tilt solar photovoltaic system (Markvart and Castañer, 2003). The energy generated per year is lower compared to the solar photovoltaic modules with single- and dual-axis tracking or maximum power point tracking (MPPT) arrangements.

2.2 Photovoltaic modules with tracking

Tracking systems in photovoltaic systems design are employed to orient solar modules by following or tracking the movement of the sun during the day, with the goal of maximizing solar energy generation (Gevorkian, 2012). These systems may be categorized as active (electrical) or passive (mechanical) type (Chin, Babu, and McBride, 2011 and Gevorkian, 2012), which can be configured to track the sun in a single- or dual-axis. Therefore, tracking systems are classified as single- or dual axis based on orientation, while they categorized as passive or active based actuation (Mousazadeh et al., 2009).

One of the features of the passive solar tracking systems is the manual adjustments of the photovoltaic modules (Chin, Babu, and McBride, 2011); such tracking systems are less complex compared to the active filters but have relatively low efficiency, and are not as widely used as the active trackers. Besides, most active tracking systems may be classified as microprocessor type, computer-controlled date and time type, auxiliary bifacial PV cell type, and a hybrid of the different types (Chin, Babu, and McBride, 2011 and Mohammad and Karim, 2013). In a microprocessor-based solar tracking system, a control system is integrated with DC motors (Chin, Babu, and McBride, 2011, and Sumathi et al., 2017) and after the site is selected, the "azimuth elevation" range is then ascertained leading to the calculation of the angular steps. In other words, the control signal which is fed to the motors provides the required tracking to be achieved (Sumathi et al., 2017). The active solar trackers offer accurate tracking and relatively high efficiency; they are widely used but they require energy supply for their operation (Sumathi et al., 2017).

In addition, there is a single-axis tilt movement in the single-axis type, while movement in regular intervals is also possible in dual-axis tracking system but can achieve adjustments for angular position (Gevorkian, 2012). The best performance is achieved in tracking systems when there is a synchronization between the tilt angle and the seasonal variations of the sun's altitude (Chin, Babu, and McBride, 2011).

Photovoltaic systems with single-axis tracking can achieve about 20 to 25% more solar energy capture than the traditional fixed tilted solar PV systems (Gevorkian, 2012). The dual-axis tracking PV systems can achieve 30 to 40% more solar power generation compared to the fixed tilted and one-axis photovoltaic modules (Markvart and Castañer, 2003 and Gevorkian, 2012). However, the dual-axis tracking system has a complex configuration than the one-axis tracking system from the mechanical point of view (Luque and Hegedus, 2011). A hybrid automatic solar tracking system reported in (Mohammad and Karim, 2013) produced 54% more power output gain compared to a fixed system that was inclined at 23.5° to the horizontal. Though the cost of tracking devices is a small proportion of the total capital costs of the photovoltaic system, they require adjustments of position on seasonal basis, system inspection and periodic lubrication of the devices of the tracking systems (Gevorkian, 2012).

The optimum operating point on the module's current-voltage (I-V) characteristics changes during the day in relation to the intermittency of the solar irradiation and the solar module's temperature (Photovoltaics Guidebook for Decision-Makers. 2003). The idea of a smart MPPT system, for instance, is that it introduces an adjustment to ensure that the operating point of the solar module is tracked where the maximum power could be obtained from the system. This kind of energy and efficiency enhancement is achieved by using power electronic converters.

Several research studies exist in the literature on the module orientation and tracking systems – one-axis, two-axis and the MPPT. However, this current study focuses on one-axis solar tracking system, and it is of interest in this section to mention some of the existing contributions relevant to the research area in addition to the contributions mentioned in the introduction. A paper has been published that considered the design and testing of a standalone one-axis active tracking device for a photovoltaic system in MATLAB/Simulink environment (Chin, Babu, and McBride, 2011). The system is made of one unit each of solar module, servo motor, battery, charger and microcontroller, including two light-dependent resistor (LDR), and an external load. The LDR was employed to sense the intensity of the sun, which then fed a signal to the microcontroller to rotate the solar module through a servo motor (Sumathi et al., 2017).

A study has also been presented that focused on global estimates of solar optimal tilt angles, including proportions of solar energy that is incident on tilted and tracked solar modules compared to the horizontal modules (Jacobson and V. Jadhav, 2018). The authors posited that the benefits of tilting and tracking increase as the latitude increases and reported different optimum tilt angles for different locations around the world. The modelling and validation of one-axis tracking system has been discussed with bifacial solar module (Pelaez et al., 2019). The authors posited that bifacial photovoltaic

modules in single-axis-tracking designs can produce 4% –15% energy gain in addition to the 15% –25% energy increase that is possible with one-axis trackers compared to the traditional fixed-tilted systems.

A work has considered the rotation angle for the optimum tracking of single-axis trackers (Marion and Dobos, 2013). The authors introduced critical equations that could be employed for designing solar radiation with appropriate tracking constraints and motor rotations to yield optimum tracking for increased energy capture. This was achieved with the consideration for the relationship the between the rotation angle, the surface tilt, and the azimuth angles. The direct tracking error characterization has been done for a single-axis tracking system (Sallaberry, et al., 2015), while the study presented in (Hafez, Yousef, and Harag, 2018) considered the review of sun trackers with focus on the technologies and the tracking mechanisms.

The existing contributions are well-appreciated as they provide relevant background for this current paper. However, this paper is focused on Fuzzy PID structures for one-axis solar photovoltaic tracking. The idea proposed by this approach is to employ the structures of Fuzzy PID as a control mechanism for the solar tracking system. A D.C. motor was modeled as the tracking system based on the Kirchhoff's laws, and the proposed PID controller was tuned using the Fuzzy logic of linear and nonlinear structures. The simulation was done in MATLAB/Simulink environment. The rise time, settling time, overshoot and peak time parameters were used for analyzing the performance of the model.

3. System Description

The solar tracking system employed permanent dc motor having a solar panel mounted on its shaft as load, which can be controlled by either a microcontroller chip or any controller circuitry. Figure 1 shows the block diagram representation of a single axis solar tracking system. The photo-resistors (LDRs) senses the sun's and solar PV current location while the comparator compares the two to generate an error signal and the controller section is housed by a microcontroller, the driver circuit serves as an actuating section as well as for provision of amplified signal for the PMDC. Research findings have shown that when solar panels are mounted in such a way that is perpendicular to sunlight at point of strongest illumination, maximum efficiency can be achieved. Furthermore, the actuator section consists of the permanent DC motor controlled by an H-bridge driver, which permits both amplification and bidirectional rotation of the motor. The permanent DC motor used in this work is a stepper motor, it allows for easy control of the PV panel. Light sensor and feedback section entail the development of an active solar tracking system for electronic circuitry built for tracking the sun's location as well as for the control of the actuator connected to the mechanism for controlling the panel. Two pairs of LDRs sense the light from the sun on the panel and gives an electrical output, which will be used to compare with the initial location of the panel. The panel position is sensed, after which it will be fed back to the comparator section of the microcontroller using a position sensor i.e. a potentiometer. Control is attained when the error between the sensed sun's location and the panel position become zero. In a dual axis solar tracker system, opaque surfaces is usually employed to provide screening of the four-light sensors LDR1 to 4, while LDR1 and LDR2 track the sun horizontally, LDR3 and LDR4 track the sun vertically (Lorenzo et al., 2002). However, for single-axis trackers, only two LDRs are required to tack the sun either vertically or horizontally. When light falls more on an LDR or pair of LDRs, the circuitry causes the panel to adjust its position so that the other LDR(s) will receive the same amount of light. The error becomes zero when all LDRs receive an equal amount of light.

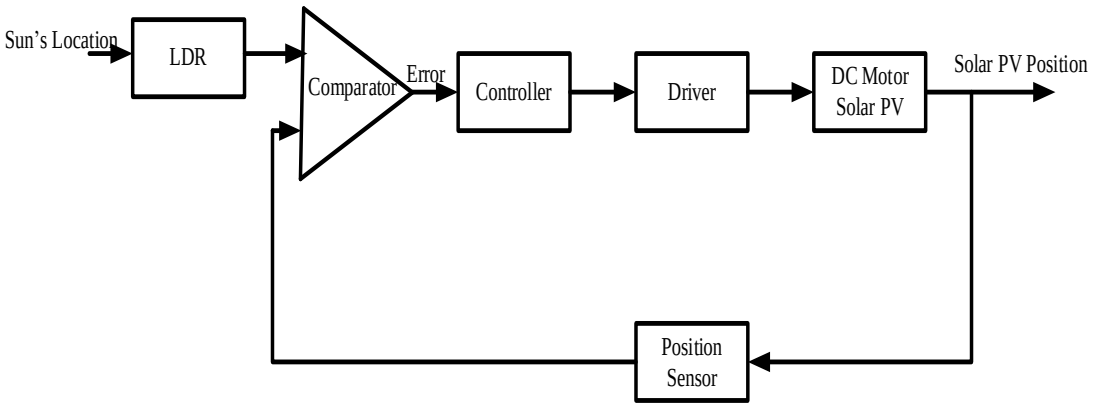

Figure 1: Block diagram of a solar tracking system

3.1 Mathematical Modeling of DC Motor and Fuzzy-PID Controller

This section deals with mathematical modelling of DC motor and fuzzy-PID controller employed for the single axis for solar tracker.

3.2 DC Motor Model

The circuit diagram representation of D.C motor is as shown in Figure 2, the input voltage is provided by the V_a to produce desired output which are the angular velocity (ω) and the shaft angle (θ). The basic governing equations of the dc motor was obtained using Kirchhoff's laws, which was latter Laplace to get equations that was used for the Simulink model of the DC motor.

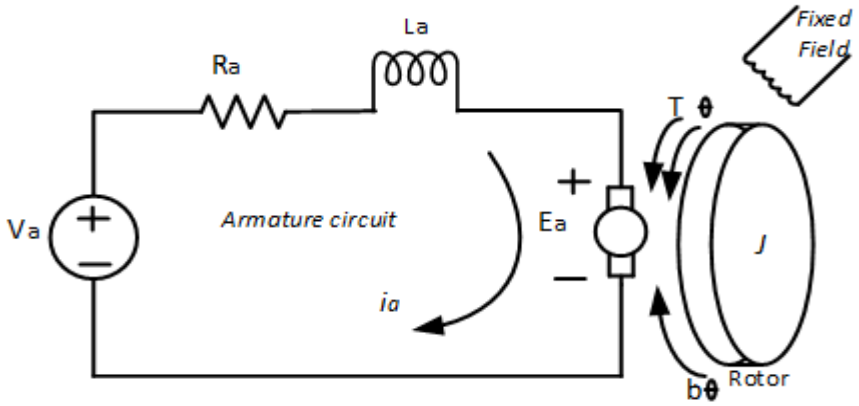

Figure 2: A schematic representation of DC Motor

Applying the Kirchhoff voltage law gives equation (1) thus;

$$V_a(t) = R_a i_a(t) + L_a \frac{di_{a(t)}}{dt} + E_b(t) \quad (1)$$

Equation (2) defines the relationship between the motor Torque, (T) and the armature current $i_a(t)$:

$$T = K i_a(t) \quad (2)$$

Similarly, the back EMF $E_b(t)$ is related to the angular velocity using equation (3):

$$E_b(t) = K\omega = K_b \frac{d\theta}{dt} \quad (3)$$

Substituting equation (3) into equation (1) gives:

$$R_a i_a(t) + L_a \frac{di_{a(t)}}{dt} = V_a(t) - K_b \frac{d\theta}{dt} \quad (4)$$

If $K_L i_a(t)$ is given as;

$$J \frac{d^2\theta}{dt^2} + b \frac{d\theta}{dt} = K_L i_a(t) \quad (5)$$

Taking Laplace transform of equations (4) and (5) gives equations (6) and (7):

$$L_a s I_a(s) + R_a I_a(s) = V_a(s) - K_b s\theta(s) \quad (6)$$

$$J_m s^2\theta(s) + B_m s\theta(s) = K_L I(s) \quad (7)$$

From equation (7) $I_a(s)$ can be expressed as in equation (8);

$$I_a(s) = \frac{V_a(s) - K_b s\theta(s)}{(R_a + L_a s)} \quad (8)$$

By substituting equation (8) into equation (7) gives equation (9) thus:

$$J_m s^2\theta(s) + B_m s\theta(s) = K_L \left(\frac{V_a(s) - K_b s\theta(s)}{(R_a + L_a s)}\right) \quad (9)$$

The transfer function $(T.F)$ defined as the ratio of the angle θ(s) to the input voltage V(s) is given thus;

$$T.F = \frac{\theta(s)}{V(s)} = \frac{K_L}{J_m L_a s^3 + (R_a J_m + L_a B_m) s^2 + (R_a B_m + K_b K_L) s} \quad (10)$$

The Simulink diagram of the DC motor modeled in equation (10) is shown in Figure 3 while the parameters of the DC motor are as presented in Table 1.

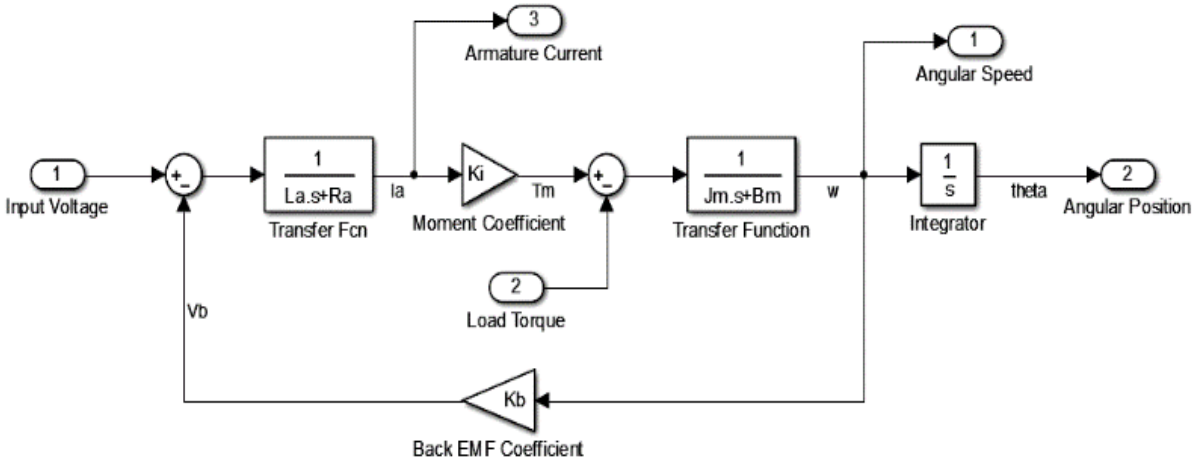

Figure 3: The Simulink Model for the DC Motor

Parameter	Description	Value
P	Power (kW)	3.70
V	Voltage (V)	240
s	Speed (r.p.m.)	1750
R_a	Armature resistance (Ω)	11.2Ω
L_a	Armature inductance (H)	0.1215
J_m	Current density (kgm^{-2})	0.02215
K_L	Spring constant (Nm/A)	1.28
K_b	Back EMF coefficient (Vs/rad)	1.28
B_m	Motor flux density (Nms/rad)	0.002953

Table 1: Parameters of the DC motor

3.3 Fuzzy-PID Controller Model

The transfer function and Simulink model for conventional PID controller as given by Ojo *et al*., (2019) is defined by equation (11) thus;

$$u(t) = K_p e(t) + K_I \int e(t)dt + K_D \frac{de(t)}{dt} \quad (11)$$

Taking the Laplace transform of equation (11), the s-domain equation expressed in equation (12):

$$U(s) = K_p E(s) + \frac{K_I}{s} E(s) + K_D s E(s) \quad (12)$$

where;

K_p= Proportional gain,

K_I = Integral gain, and

K_D = Derivative time

K_D *is* used to tune the motor of the solar tracking system modeled in equation (10) while Figure 4 shows the PID controller Simulink model in equation (11):

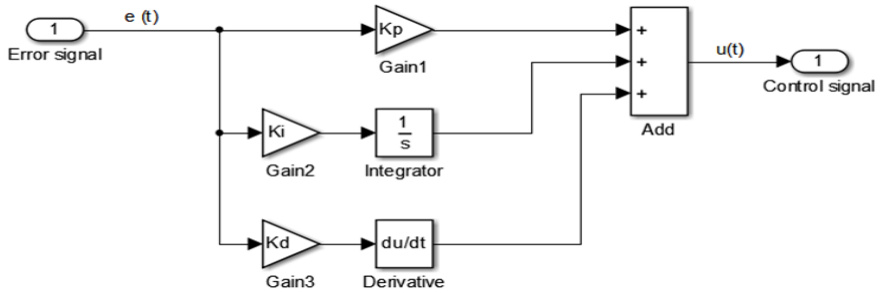

Figure 4: Simulink model for traditional PID controller

Fuzzy logic is incorporated into the modeled PID controller to get Fuzzy-PID controller with a view to achieve effective tuning of the controller proposed for this work. The Fuzzy PD+I type controller structure shown in Figure 5 was employed in this work. This type uses the PID parameters to generate its own gains used to tune the plant. It converts the linear property of the conventional PID to a linear Fuzzy and finally to linear Fuzzy-PID. The linear Fuzzy-PID is converted to the nonlinear type that uses fuzzy-PI and fuzzy-PD controllers in tandem as shown in Figure 6 using a modified procedure presented by MathWorks (2002 - 2011) with a view to improve the system response. It is in the feedback loop mode working like a PID controller but through a fuzzy inference system. The procedures for incorporating the Fuzzy logic into the PID controller include fuzzification, rule base, inference mechanism, and defuzzification as discussed in the subsequent subsections.

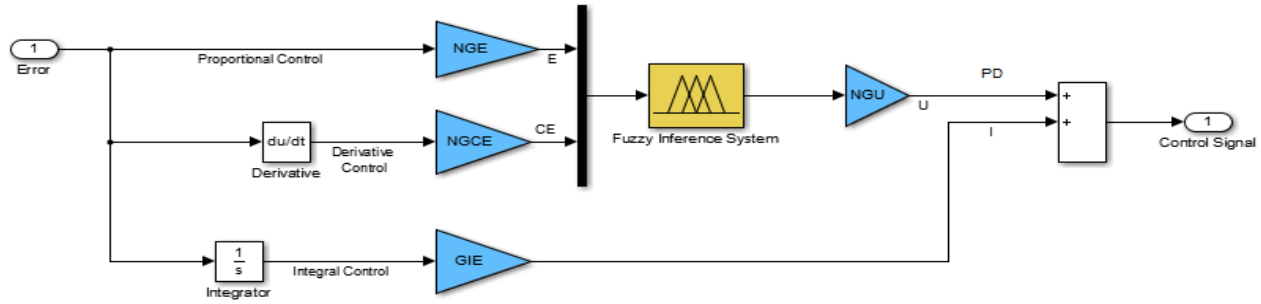

Figure 5: Fuzzy PD+I structure simulink model

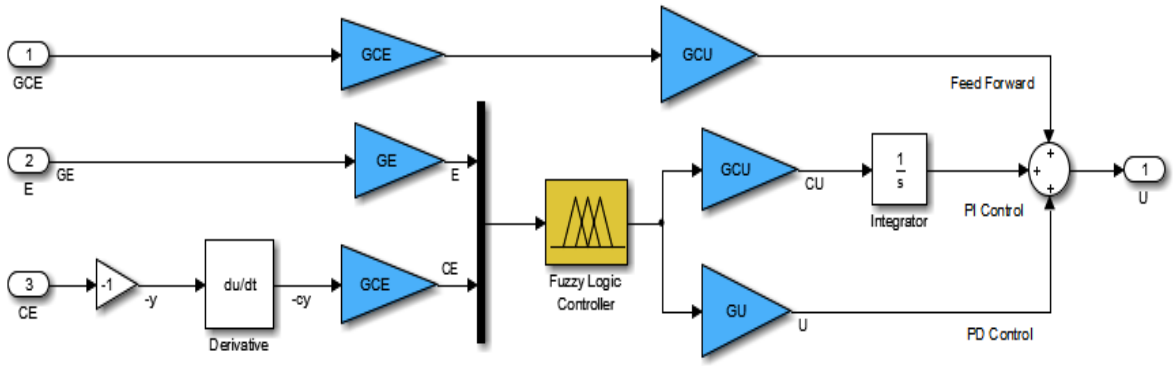

Figure 6: Fuzzy PI+PD structure Simulink model

3.3.1 The Fuzzy Inference System

From Figure 6, the Fuzzy-PID structure consists of two input variables; error (E) and error derivative (CE) and one output variable being the control signal (U). These input variables via the fuzzy inference system (FIS) serve as the input variable for the fuzzification process while the FIS output U(t) is the control signal generated from the fuzzy rules. If the desired angle of the DC motor is $r(t)$ and the actual angle is $y(t)$ then, the error can be expressed as in equation (13) thus;

$$e(t) = r(t) - y(t) \tag{13}$$

where;

$e(t)$ = error (expected to be zero)

The derivative of $e(t)$ is defined by equation (14) thus;

$$\Delta e(t) = \frac{de(t)}{dt} \tag{14}$$

Based on Figure 6, the crisp inputs are $e(t)$ and $\Delta e(t)$, which correspond to E and CE (the error and error derivative), respectively. The crisp inputs are converted with the aid of fuzzification interface into the fuzzy membership values that are used in the rule base to execute the related rules to generate an output [39]. The configuration of the fuzzy inference system was done based on the following steps:

- Mamdani style FIS was used,
- range of the both inputs were chosen to be (-60 60),
- triangular input sets were used and cross neighbor sets at membership value of 0.5,
- the range for the Output was chosen to be (-240, 240),
- algebraic product for AND connective was employed.
- singleton was used as output.
- defuzzification method used is the Centre of Gravity method (COG).

The interfaces generated based on the above listed steps were as shown in Figures 7 and 8 for FIS inputs and output, respectively. From the Figures, it can be inferred, that each input (E and CE) has three (3) membership functions namely; Negative (NEG), Zero (ZE), and Positive (POS) with a triangular shape and the Output make use of five (5) membership functions, which are Negative Big (NB), Negative Small (NS), Zero (Z), Positive Small (PS) and Positive Big (PB) with singletons values. In this work, for a step input, the range of the two inputs E and CE are set as -1, 1 while the output is set as -10, 10. These membership functions were used in the next section to generate Fuzzy rules.

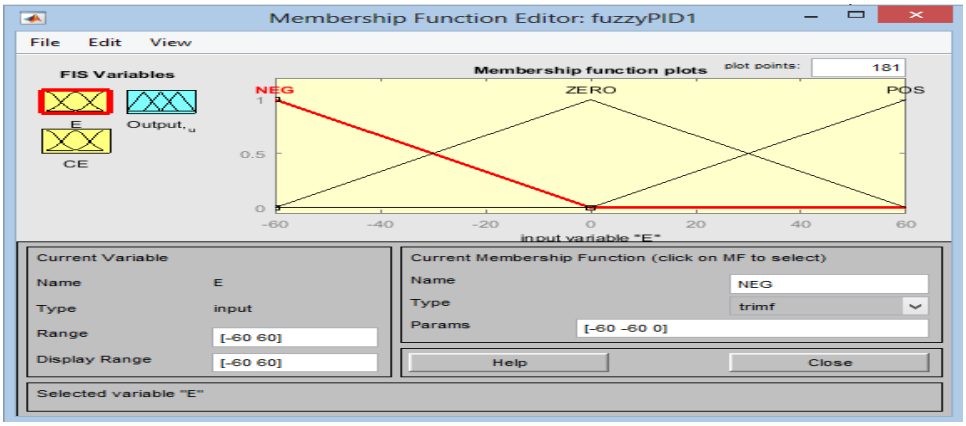

Figure 7: FIS Inputs (C and CE) of Fuzzy PI+PD membership functions

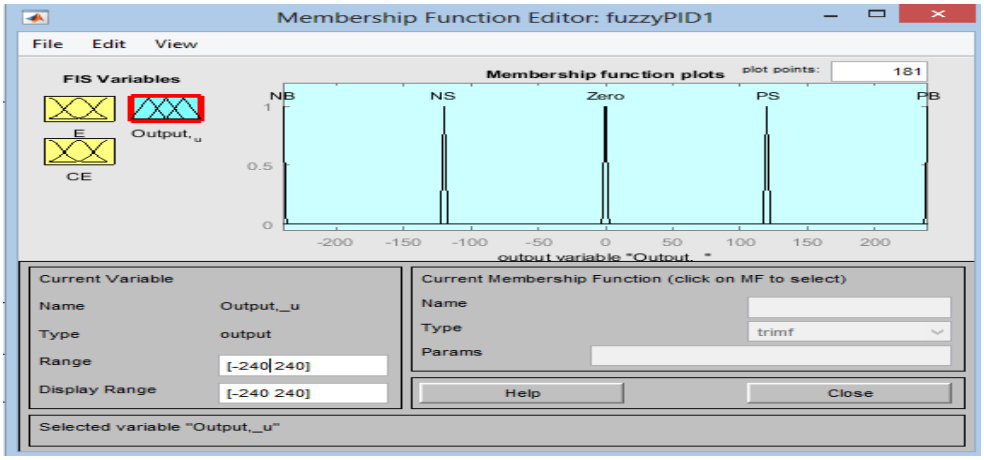

Figure 8: FIS Output (u) of Fuzzy PI+PD membership functions

3.3.2 The Fuzzy Rule Structure

A set of fuzzy linguistic rules that produces a fairly accurate decision similar to human's manner required for the controller to operate on. The fuzzy rule structure employed in this work is made up of 9 sets of rules stated as follows and represented using Figure 9

i). U assumed the status of NB once E and CE is NEG
ii). U assumed the status of NS, once E is NEG and CE is ZE
iii). U assumed the status of ZE, once E is NEG and CE is POS
iv). U assumed the status of NS, once E is ZE and CE is NEG
v). U assumed the status of ZE, once E is ZE and CE is ZE
vi). U assumed the status of PS once E is ZE and CE is POS
vii). U assumed the status of ZE, once E is POS and CE is NEG
viii). U assumed the status of PS, once E is POS and CE is ZE
xi). U assumed the status of PB once E is POS and CE is POS

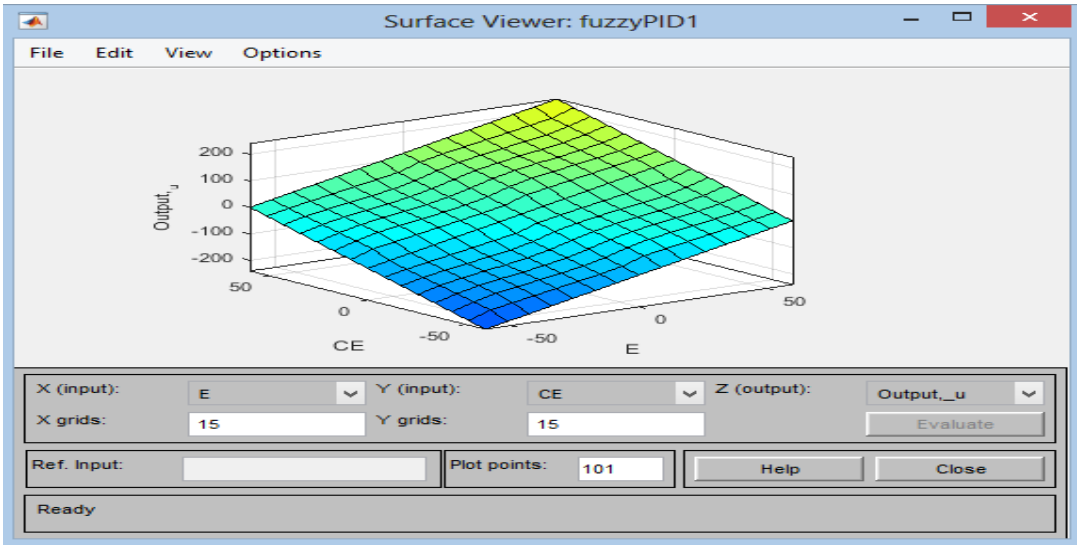

Figure 9: Surface view of the fuzzy rules of Fuzzy PI+PD

These rules are implemented in a non-linear fuzzy PI + PD parallel structure, which uses the Sugeno inference system and Gaussian membership function for the fuzzification consisting of two inputs (E and CE). The Simulink model of this structure is as presented in Figure 6 where the second input to the fuzzy inference system is taken from the output of our plant i.e. y instead of the normal change in error.

3.3.3 Determination of the Scaling Factors

The scaling factors for the Fuzzy PD+I linear structure are NGE, NGCE, GIE, and NGU which are related to the conventional PID parameters as in equations (15) to (17):

$$NGCE = (NGE * K_D)/K_p \quad (15)$$

$$GIE = (NGE * K_i)/K_p \quad (16)$$

$$NGU = NGE/K_p \quad (17)$$

The Value of NGE depends on the range of error and the universe of the Inputs of the FIS. For the Non – linear Fuzzy PI+PD structure, the scaling parameters are GE, GCE, GCU, GU and are determined from the conventional PID parameters (K_p, K_i, K_D) using the following equations below:

$$K_p = GCU * GCE + GU * GE \quad (18)$$

$$K_i = GCU * GE \quad (19)$$

$$K_D = GU * GCE \quad (20)$$

Table 2 was realized based on the tuning procedures discussed in the previous sections.

Table 2: Tuning parameters of the controllers

3.3.4 Input section of the Model

The input section of the model is actually the altitude angle of the current sun's location as tracked and calculated. For this work, the input to the solar tracker model for simulation purposes was chosen to be the calculated altitude angle of Sun's trajectory in Ogbomoso. This angle as a function time was used as the set point, while a unit step function was employed to test the model and finally, a signal builder was used to produce a signal that mimics angular input analogous to the sun altitude angle. The sun data of 23rd December 2019, for Ogbomoso, Oyo State, Nigeria is depicted in Figure 10 and from the Figure, the data in Table 3 were obtained.

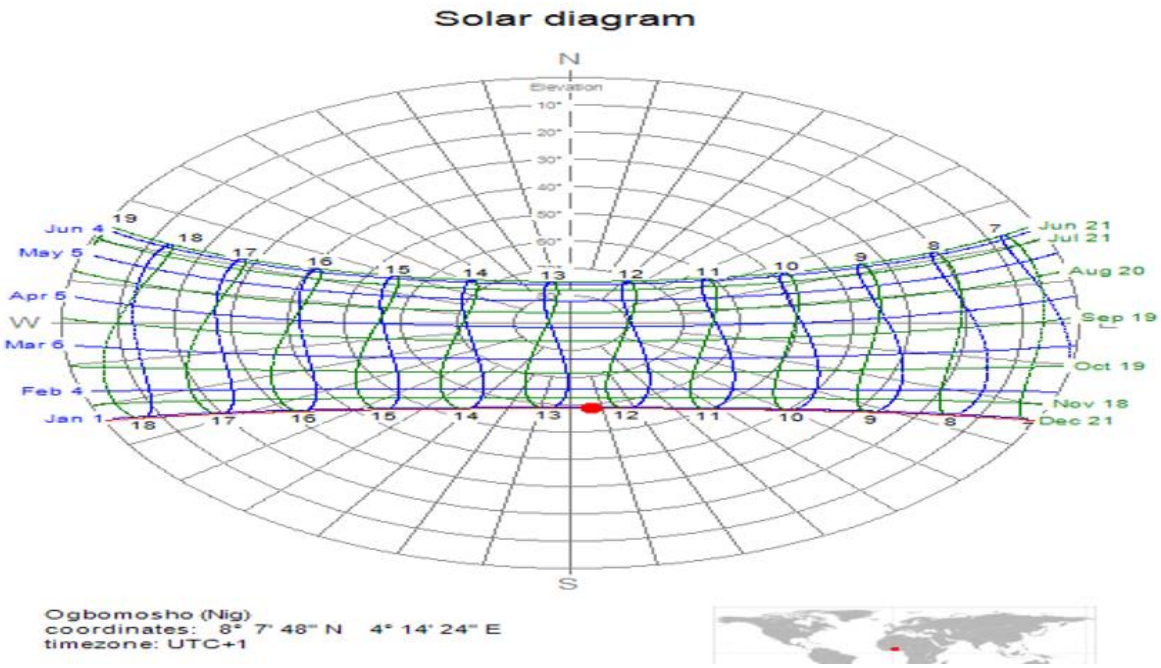

Controller/Parameters	K_p	K_i	K_d	GE	GCE	GIE	GCU	GU	K
PID	0.42	0.702	0.05	-	-	-	-	-	2.5
Fuzzy PD+I	0.42	0.702	0.05	3	0.112	66	-	30	1
Fuzzy PI+PD	0.42	0.702	0.05	10	1.64	-	0.0702	0.0305	2.6

Figure 10: A sample data of Sun details of Ogbomoso, Oyo State, Nigeria.

Solar Parameter	Value

Azimuth angle	172.26°
Elevation angle or altitude angle	58.20°
Latitude	8°7’48”N
Longitude	4°14’24”E
Sunrise	06:52
Sunset	18:31
Solar noon	12:42

Table 3: Solar parameter value

From Table 3, the number of sunshine hours was found to be:

$$18:31 - 6:29 = 12hrsapprox. \quad (21)$$

The position sensor is simply a potentiometer and its constant K_{pot} was found using equation (22) was used as feedback for the overall design;

$$V_p = \theta_L \times K_{pot} = \frac{VoltageChange}{DegreeChange} \quad (22)$$

The solar panel was not modeled but it was rather represented with a step input/constant block in the Matlab/Simulink during simulation stage. Solar tracking system open-loop Simulink model as well as the overall Simulink diagram with the three controllers are depicted with Figures 11 and 12, respectively.

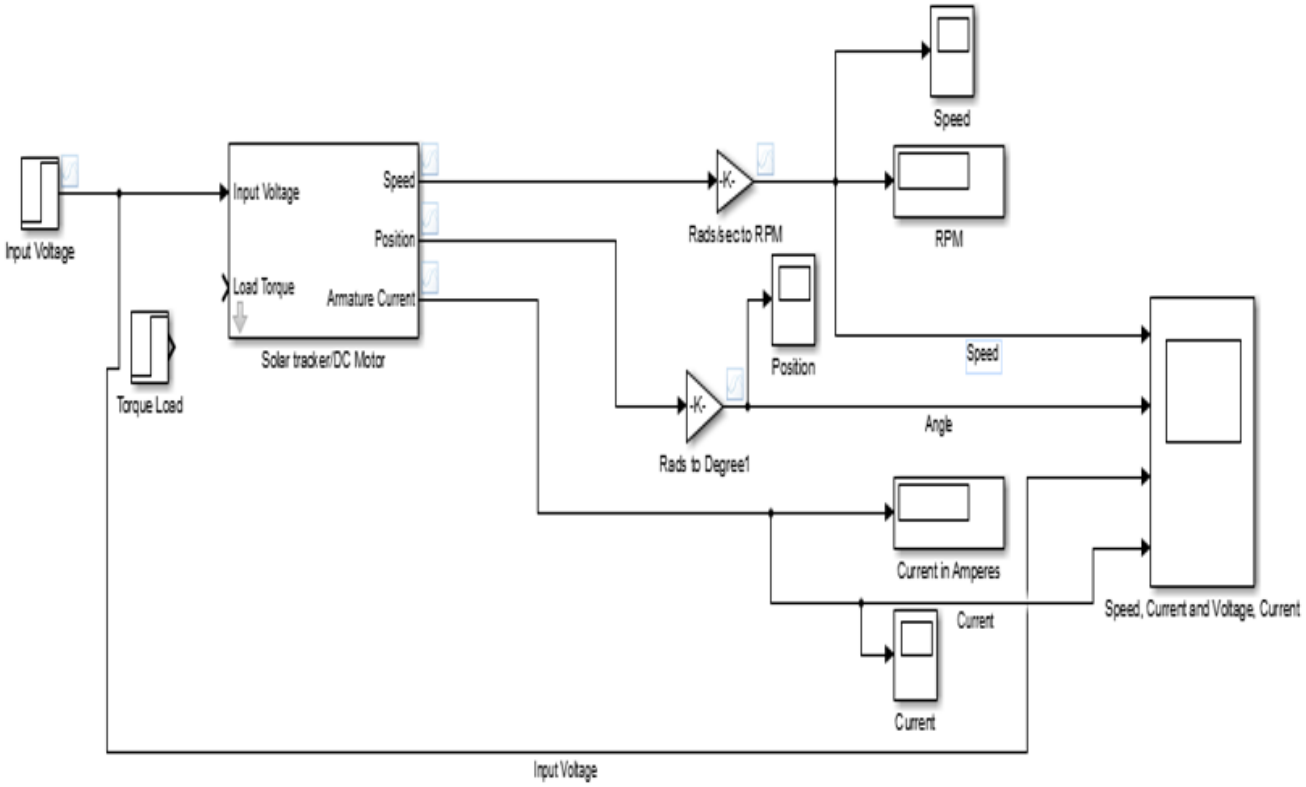

Figure 11: Open-loop Simulink model

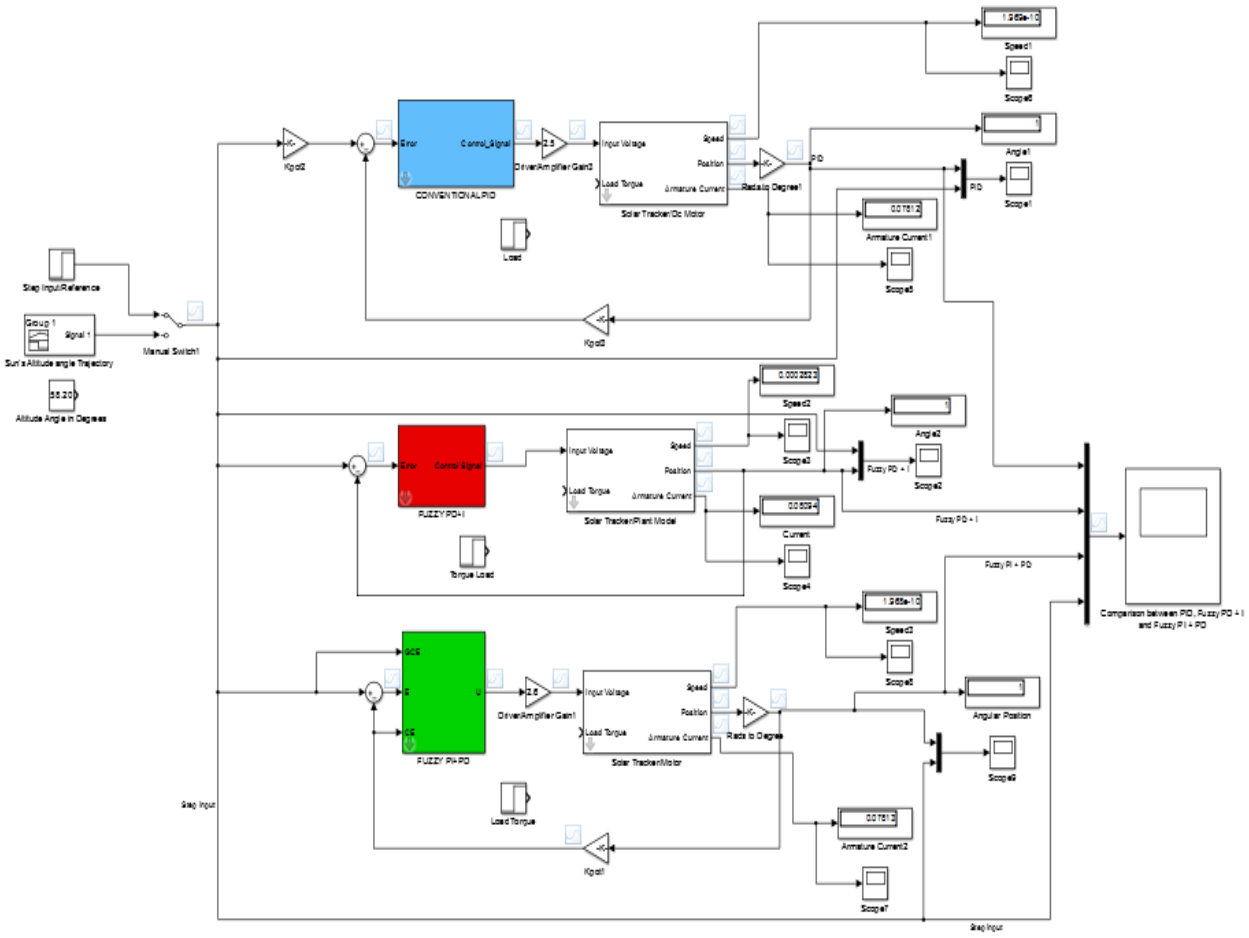

Figure 12: Overall Simulink model with three controllers for the solar tracking system.

4. Simulation Results

This section presents the simulation results obtained for single axis solar tracking system based on Fuzzy-PID controller, the results of the open-loop test on solar tracking system was as depicted by Figures 13 through 18. The results of open-loop speed response of solar tracker on no-load is depicted by Figure 13 which shows that the speed was found to be approximately 1755 rpm when there is no load on the system. Figure 14 shows that an open-loop current of about 0.4A was drawn by the system when there is no load acting on it. In Figure 15, the open-loop speed with a load of 0.1 Nm is presented and the Figure showed that the speed is around 1627.2 rpm which indicates a significant reduction when compared with Figure 13. Also, the open-loop current with a load of 0.1 Nm was presented in Figure 16 where a current of about 2A was drawn by the system and this indicates a significant increase when compared with Figure 14. The input voltage of 240V and the maximum angle of the system was as shown with Figures 17 and 18, respectively.

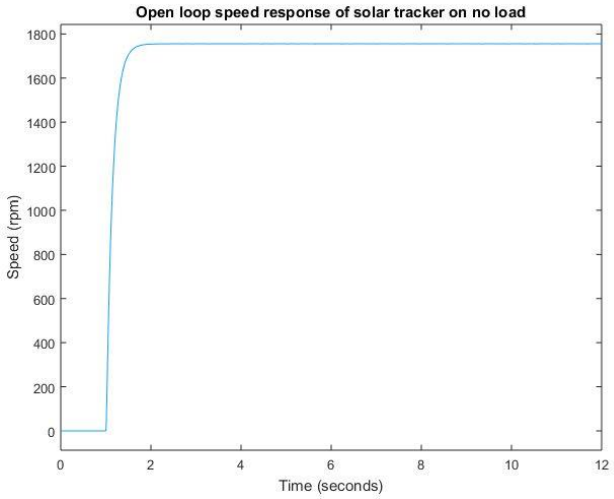

Figure 13: Open Loop No Load Speed

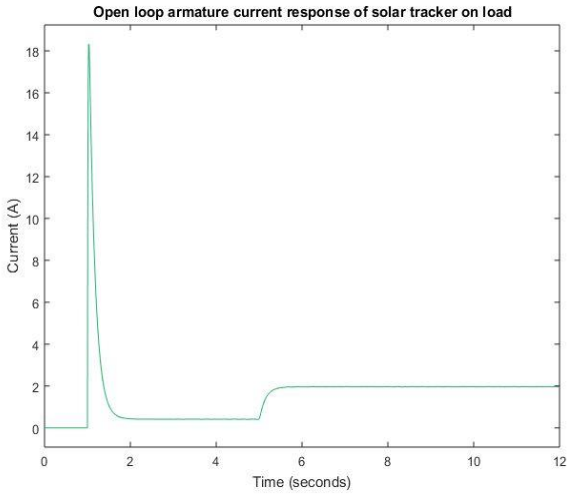

Figure 16: Open Loop Current with 0.1 Nm Load

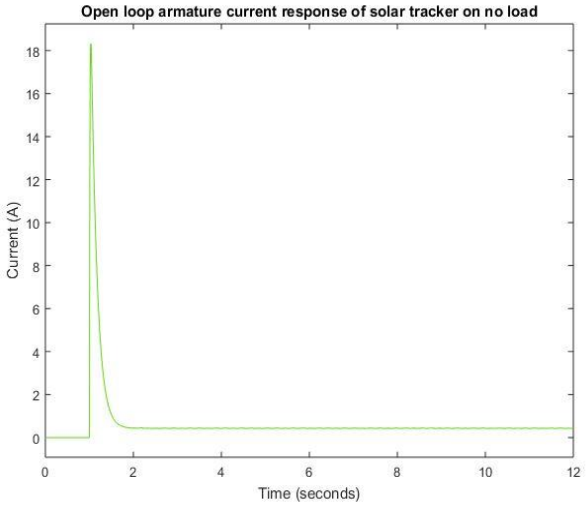

Figure 14: Open Loop No Load Current

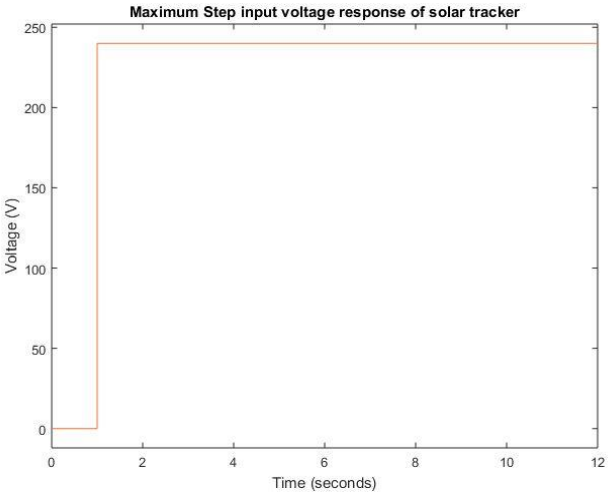

Figure 17: Open Loop Input Voltage

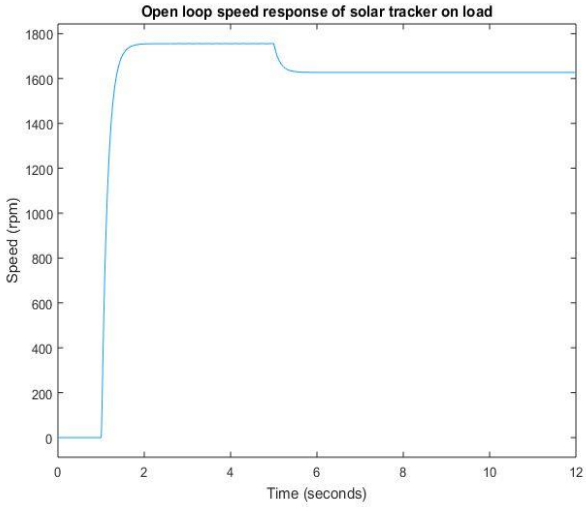

Figure 15: Open Loop Speed with 0.1 Nm Load

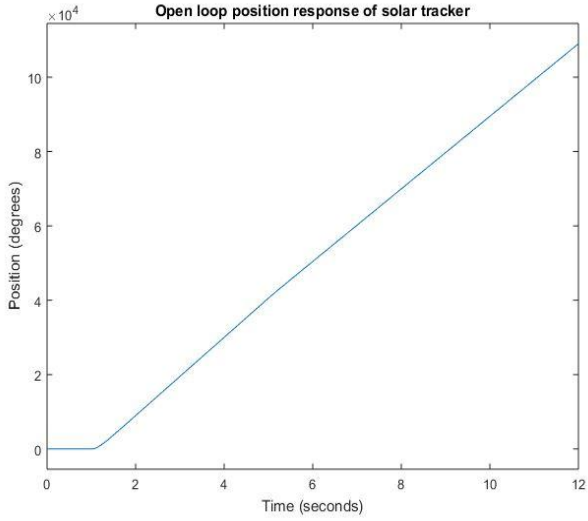

Figure 18: Open Loop Maximum Angle

The closed-loop response of the system on a load of 0.1Nm was as shown in Figures 19 through 22. In Figure 19, the closed-loop current with PID controller when a load of 0.1Nm act on the system was found to be 1.68A and the Figure showed that the system oscillates more though within 0.4s time frame. The closed-loop on load speed response with PID controller was presented in Figure 20 where the reference speed is 500 rpm with an overshoot of 12.4 rpm and this speed was found to have dropped to 438.3 rpm when subject to a load of 0.1 Nm. The comparison of motor angle for different controllers under no-load condition is presented in Figure 21 and the Figure showed that the Fuzzy PD + I controller is better in terms of rise time and peak amplitude of 1.15s and 1.43s, respectively.

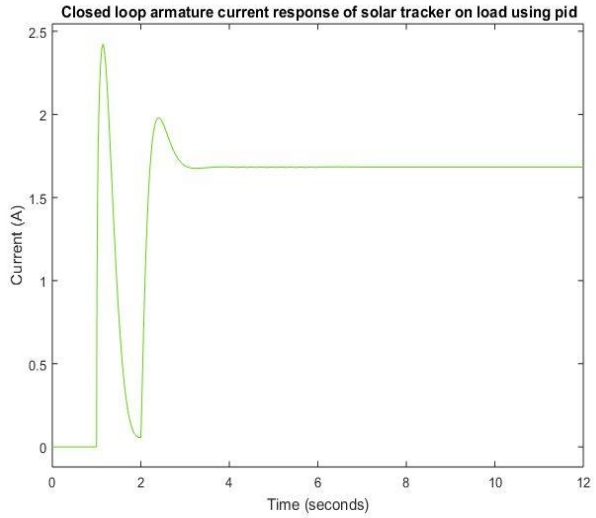

Figure 19: Closed Loop on Load Current

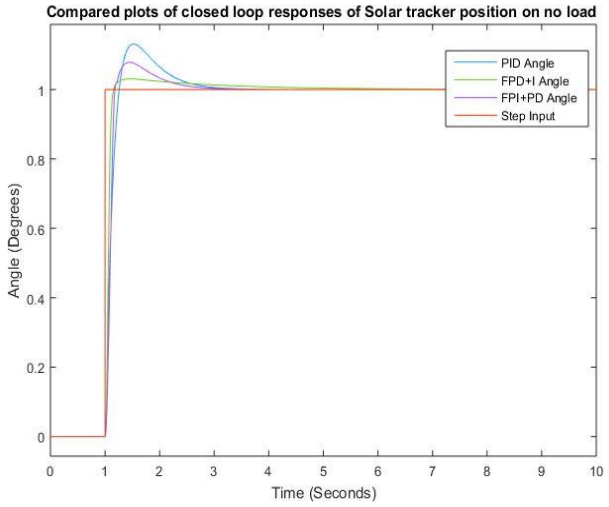

Figure 21: Comparison of the controllers at no load

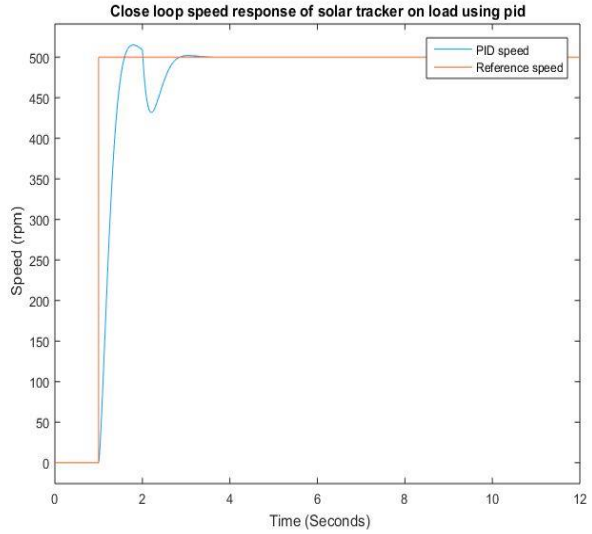

Figure 20: Closed Loop on Load Speed

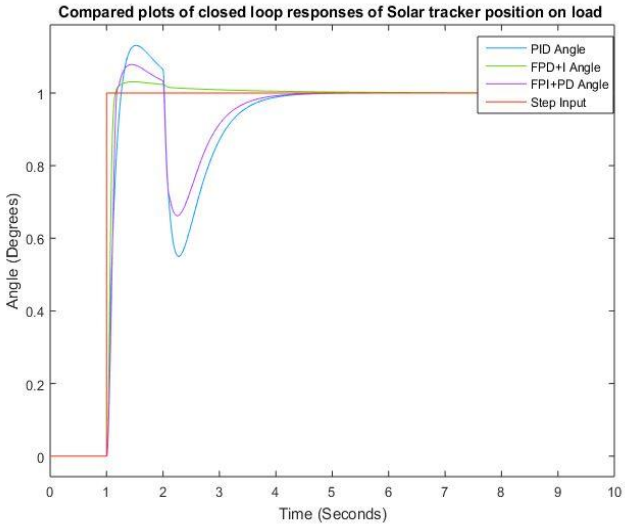

Figure 22: Comparison of the controllers under load

The comparison of motor angle for different controllers when the system is subjected to a load of 0.1 Nm is presented in Figure 22 and the Figure showed that Fuzzy PD + I controller is better in terms of rise time and peak amplitude of the same value of 1.15s and 1.43s, respectively, like that of no-load condition.

The mimicked response of 12hours sunrise time (sun's trajectory) with maximum altitude angle of 58.20° is shown in Figure 23 and it is observed from the Figure that the sun's trajectory was accurately tracked by the fuzzy PD+I and PID controller with minimal error and quick response.

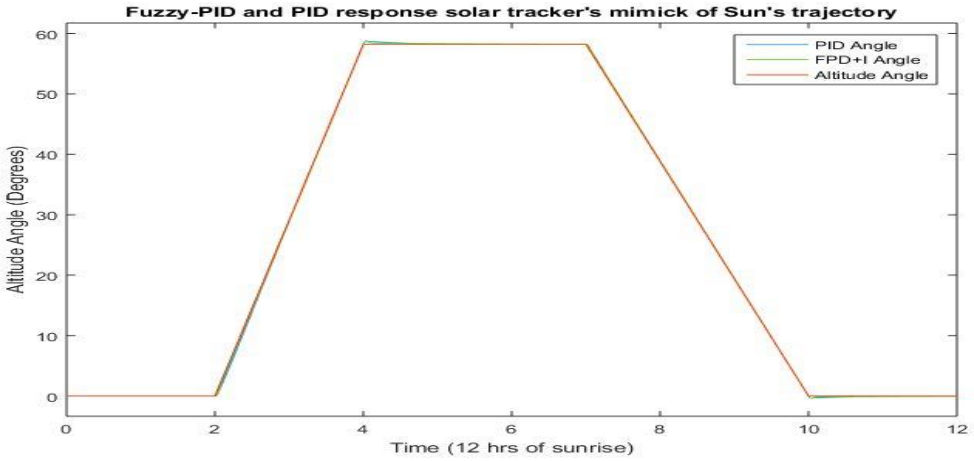

Figure 23: Mimicked response of the solar tracker on a 12hrs sun's position

Table 4 presented the performance evaluation of the system when it is subjected to no-load, and the results revealed that the Fuzzy PD + I controller performed better in terms of rise time of 1.15s when compared to that of conventional PID and Fuzzy PI + PD controllers of 1.25s and 1.17s, respectively. Also, it can be inferred that the Fuzzy PI + PD controller is better in terms of settling time of 2.87s while the Fuzzy PD + I controller is considered best in terms of overshoot of 3% when compared to others. In addition, Fuzzy PD + I controller performed well in terms of peak time of 1.43s when compared to conventional PID and Fuzzy PI + PD controllers.

Performance metrics	PID	Fuzzy PD + I	Fuzzy PI + PD
Rise time (s)	1.25	1.15	1.17
Settling time (s)	3.10	3.53	2.87
Overshoot (%)	13	3	8
Peak time (s)	1.50	1.43	1.46

Table 4: System performance at no load condition

The performance evaluation of the system at loading condition was as presented in Table 5. Fuzzy PD + I controller performed better in terms of rise time and the peak time of 1.15s and 1.43s, respectively, which when compared to the results presented in Table 4 showed that there is no significant difference in rise time and peak time when the system is subjected to 0.1 Nm load. Also, from Table 5, it can be deduced that the Fuzzy PD + I controller is better in terms of settling time and overshoot of 3.15s and 3%, respectively. Finally, it can be generally observed from the results presented thus far that the Fuzzy PD + I controller performed better when subjected to a load of 0.1 Nm.

Performance metrics	PID	Fuzzy PD + I	Fuzzy PI + PD
Rise time (s)	1.25	1.15	1.17
Settling time (s)	4.57	3.15	4.55
Overshoot (%)	13	3	8
Peak time (s)	1.53	1.43	1.46

Table 5: System performance at a load of 0.1Nm

5. Conclusion

An investigative study on a PID controller tuned by Fuzzy logic of different structures such as conventional PID, Fuzzy PD + I and Fuzzy PI + PD was designed, mathematically modeled and simulated in Matlab/Simulink environment. The performance of the system was evaluated using rise time, settling time, overshoot, and peak time as metrics. The simulation results generally revealed that the Fuzzy PD + I controller structure outperformed the conventional PID and Fuzzy PI + PD controller structures when subjected to no-load and when subjected a load of 0.1 Nm. From the comparison of Fuzzy PD+I and Fuzzy PI + PD, it is clear that both controller structures offer close responses and control of the plant as compared to the conventional PID controller. Further work will focus on the effect of solar panel sizing on the control performance of the system solar tracking system.

References

Abdallah S., (2004) The Effect of using Sun Tracking Systems on the Voltage–Current Characteristics and Power Generation of Flat Plate Photovoltaics. Energy Conversion and Management, 45: 1671–1679.

Abdullahi D., Suresh S., Renukappa S., and Oloke D., (2017). Key Barriers to the Implementation of Solar Energy in Nigeria: A Critical Analysis. IOP Conference Series: Earth and Environmental Science, 83(2017):1-8.

Adusei L. (2012). Energy security and the future of Ghana. Accessed 3 July 2020. Available at: http://newsghana.com.gh/energy-security-and-the-future-of-ghana/

Bada H, A. (2011) Managing the Diffusion and Adoption of Renewable Energy Technologies in Nigeria. World Renewable Energy Congress, Linkoping, Sweden, 2642–2649.

Bakos G. C. (2006) Design and Construction of a Two-Axis Sun Tracking System for Parabolic Trough Collector (PTC) Efficiency Improvement. Renewable Energy, 31: 2411–2421.

Batayneh, W., Owais A., and Nairoukh M., (2013) An Intelligent Fuzzy Based Tracking Controller for a Dual-axis Solar PV System. Automatic in Construction, 29: 100–106.

Brooks W. and Dunlop J., (2012) "Photovoltaiv (PV) Installer Resource Guide," *NABCEP*, 5.3: 1-162.

Chamanpira M., Ghahremani M., Dadfar S., Khaksar M., Rezvani A. and Wakil K. (2019) A Novel MPPT Technique to Increase Accuracy in Photovoltaic Systems under Variable Atmospheric Conditions using Fuzzy Gain scheduling. Energy Sources, Part A: Recovery, Utilization, and Environmental Effects, 1 – 23.

Chin C. S. Babu A., and McBride W., (2011) "Design, modeling and testing of a standalone single axis active solar tracker using MATLAB/Simulink," Renewable Energy, 36, 11: 3075–3090.

Dhanabal R., Bharathi V., Ranjitha R., Ponni A., Deepthi S., and Mageshkannan P., (2013) Comparison of Efficiencies of Solar Tracker Systems with Static Panel Single Axis Tracking System and Dual Axis Tracking System with Fixed Mount. International Journal of Engineering and Technology, 5: 1925–1933.

El Kadmiri Z., El Kadmiri O., Masmoudi L., and Bargach M. N. (2015). A Novel Solar Tracker Based on Omnidirectional Computer Vision. Journal of Solar Energy, 1-6.

Eshun M.E. and J. Amoako-Tuffour (2016). A Review of the Trends in Ghana's Power Sector. Energy Sustainable and Society, 6: 9-16

Gama A., Larbes C., Malek A., Yettou F., and Adouane. B. (2013). Design and Realization of a Novel Sun Tracking System with Absorber Displacement for Parabolic Trough Collectors. Journal of Renewable and Sustainable Energy, 5: 033108-18.

Gevorkian P., (2012), Alternative Energy Systems in Building Design. 2012.

Guaita-Pradas I., Marques-Perez I., Gallego A., and Baldomero S., (2019) Analyzing Territory for the Sustainable Development of Solar Photovoltaic Power Using GIS Databases. Environ Monit Assess, 191:764-781.

Hafez A. Z., Yousef A. M., and Harag N. M., (2018) "Solar tracking systems: Technologies and trackers drive types – A review," *Renewable and Sustainable Energy Reviews*, 91: 754–782.

International Energy Agency. (2014). World Energy Outlook Special Report. Retrieved August 17, 2020 from http:// www.iea.org/publications/freepublications/publication/

Jacobson M. Z. and Jadhav V. (2018), "World estimates of PV optimal tilt angles and ratios of sunlight incident upon tilted and tracked PV panels relative to horizontal panels," Sol. Energy, 169: 55–66

Jiang B., Karimi H., Kao Y, and Gao C (2018). A Novel Robust Fuzzy Integral Sliding Mode Control for Nonlinear Semi-Markovian Jump T–S Fuzzy Systems. IEEE Transactions on Fuzzy Systems, *26*:3594–3604

Kabalci E., Calpbinici A. and Y. Kabalci Y. (2015). A Single-Axis Solar Tracking System and Monitoring Software. International Conference – 7th Edition Electronics, Computers and Artificial Intelligence, Bucharest, România: 1-21.

Kiyak E. and Gol G., (2016) A Comparison of Fuzzy Logic and PID Controller for a Single-Axis Tracking System. Renewables: Wind, Water, and Solar, 3:1–14.

Li D. H. W. and Lam T. N. T. (2007). Determining the Optimum Tilt Angle and Orientation for Solar Energy Collection Based on Measured Solar Radiance Data. International Journal of Photo Energy, 1–10.

Li H., Zhao C., Wang H., Xie S., and Luo J. (2014). An improved PV system based on dual-axis solar tracking and MPPT. Proceedings of 2014 IEEE International Conference on Mechatronics and Automation, Tianjin, China.

Liu L., Han X., Liu C., and Wang J., (2013). The Influence Factors Analysis of the Best Orientation Relative to the Sun for Dual-Axis Sun Tracking System. Journal of Vibration and Control, 21: 328–330.

Lorenzo E., Perez M., Ezpeleta A., and Acedo J., (2002) "Design of Tracking Photovoltaic Systems with a Single Vertical Axis. Progress in Photovoltaic". Research and Applications, 1: 533–543.

Louchene A., Benmakhlouf A., and Chaghi A. (2007). Solar Tracking System with Fuzzy Reasoning Applied to Crisp Sets. Revue des Energies Renouvelables, 10: 231 – 240.

Luque A. and Hegedus S., (2011). Handbook of Photovoltaic Science and Engineering, 1-178.

Mahfouz A. A., Aly A. A., and Salem F. A., (2013) Mechatronics Design of a Mobile Robot System. International Journal Intelligent Systems and Applications, 5:23-36.

Mardlijah G., Zhai D., Adzkiya L, Mardianto and Ikhwan M. (2009) Modified T2FSMC approach for solar panel systems, Systems Science and Control Engineering, 7: 189-197

Marion W. F. and Dobos A. P., (2013) "Rotation Angle for the Optimum Tracking of One-Axis Trackers," Nrel, 2013.

Markvart T. and L. Castañer L., (2003) Practical Handbook of Photovoltaics: Fundamentals and Applications. 2003.

Merheb A. R., Noura H., and Bateman F., (2015) Design of Passive Fault-Tolerant Controllers of a Quadrotor Based on Sliding Mode Theory. *International Journal of Applied Mathematics and Computer Science*, *25*, 561–576.

Mohammad N. and Karim T. (2013), "Design and implementation of hybrid automatic solar-tracking system" International Journal of Electrical and Power Engineering, 6:111-117.

Mousazadeh H., Keyhani A., Javadi A., Mobli H., Abrinia K., and Sharifi A., (2009). "A review of principle and sun-tracking methods for maximizing solar systems output," Renewable and Sustainable Energy Reviews. 3:1800–1818.

Ojo, K. E., Amole, A. O., Aborisade, D. O. and Okelola, M. O. (2019), "Fuzzy-PID based Speed-Torque Control of Switched Reluctance Traction Motor", Automatic Control and System Engineering Journal, ICGST, 19(2): 31-41.

Owusu P. A. and Asumadu-Sarkodie S. (2016) A Review of Renewable Energy Sources, Sustainability Issues and Climate Change Mitigation. Cogent Engineering, 3: 1167-1190.

Oyedepo S. O. (2012) Energy and Sustainable Development in Nigeria: The Way Forward. Energy Sustainable and Society, 2:15-32.

Panwar N., Kaushik S., and Kothari S. (2011) Role of Renewable Energy Sources in Environmental Protection: A Review. Renewable and Sustainable Energy Reviews, 15:1513–1524

Pei P., Pei Z., Tang Z., and Gu H., (2018) Position Tracking Control of PMSM Based on Fuzzy PID-Variable Structure Adaptive Control. Applied Mathematics for Engineering Problems in Biomechanics and Robotics, 1-15

Pelaez S. A., Deline C., Greenberg P., Stein J. S., and Kostuk R. K., (2019) "Model and Validation of Single-Axis Tracking with Bifacial PV," IEEE J. Photovoltaics, :1-7.

Photovoltaics Guidebook for Decision-Makers. 2003, 1-278.

Racharla S. and K. Rajan K. (2017). Solar Tracking System – A Review, International Journal of Sustainable Engineering, 10: 72-81.

Rahman S., Ferdaus R. A., Mannan M. A., and Mohammed M. A. (2013). Design and Implementation of a Dual Axis Solar Tracking System. American Academic and Scholarly Research Journal, 5: 47–54.

Roth P., Georgiev A., and Boudinov H. (2005). Cheap Two Axis Sun Following Device. Energy Conservation and Management, 46:1179 -1192.

Sahoo J., Samanta S., and Bhattacharyya S., (2018). Adaptive PID Controller with P&O MPPT Algorithm for Photovoltaic System. IETE Journal of Research, 1–12.

Sallaberry F. Pujol-Nadal R., Larcher M., and Rittmann-Frank M. H., (2015) "Direct tracking error characterization on a single-axis solar tracker," Energy Convers. Manag., 105:1281–1290.

Samantaa A., Duttab A., and Neogic S. (2012) A Simple and Efficient Sun Tracking Mechanism Using Programmable Logic Controller. Applied Solar Energy, 48(2012): 218–227.

Shaaban M. and Petinrin J. O. (2014) Renewable Energy Potentials in Nigeria: Meeting Rural Energy Needs. Renewable and Sustainable Energy Reviews, 29: 72–84.

Sumathi V., Jayapragash R., Bakshi A., and Kumar Akella P., (2017) "Solar tracking methods to maximize PV system output – A review of the methods adopted in recent decade," Renewable and Sustainable Energy Reviews, 74:130–138.

Tiwari G, N. and Mishra N. K. (2011). Advanced Renewable Energy Sources. Royal Society of Chemistry, 1-9.

Usta M. A., Akyaszi O., and Atlas I. H. (2011). Design and Performance of Solar Tracking System With Fuzzy Logic Controller. 6th International Advanced Technologies Symposium (IATS'11), 16-18 May 2011, Elazığ, Turkey.

Yilmaz S., H. R. Ozcalik H. R., Dogmus O., Dincer F., Akgol O., and Karaaslan M., (2015) Design of Two Axes Sun Tracking Controller with Analytically Solar Radiation Calculations. Renewable and Sustainable Energy Reviews, 43: 997–1005.